Development of Hydro-Meteorological Hazard Early Warning System in Indonesia

Armi Susandi[1*], Mamad Tamamadin[1], Alvin Pratama[2], Irvan Faisal[2], Aristyo R. Wijaya[1], Angga F. Pratama[1], Olgha P. Pandini[3] & Destika Agustina Widiawan[3]

[1]Department of Meteorology, Faculty of Earth Sciences and Technology, Institut Teknologi Bandung, Jalan Ganesha No. 10, Bandung 40132, Indonesia
[2]Department of Environmental Engineering, Faculty of Civil and Environmental Engineering, Institut Teknologi Bandung, Jalan Ganesha No. 10, Bandung 40132, Indonesia
[3]Department of Oceanography, Faculty of Earth Sciences and Technology, Institut Teknologi Bandung, Jalan Ganesha No. 10, Bandung 40132, Indonesia
*E-mail: armi@meteo.itb.ac.id

Abstract. This paper discusses the result of the development of a hydro-meteorological hazard early warning system (H-MHEWS) that combines weather prediction from Weather Research and Forecasting (WRF) and the hydrometeorological hazard index from the National Disaster Management Authority (BNPB), Indonesia. In its current development phase, the hazards that H-MHEWS predicts are floods, landslides, and extreme weather events. Potential hazard indices are obtained by using an overlay approach and resampling so that the data have a 100-m spatial resolution. All indices are classified into 4 status categories: “No alert”, “Advisory”, “Watch”, and “Warning”. Flood potential is produced by overlaying rainfall prediction at 3-hour intervals with the flood index. Landslide potential is produced by overlaying rainfall prediction with the landslide index. Extreme weather potential is divided into 3 categories, i.e. heavy rain, strong winds, and extreme ocean waves. The whole prediction is dynamic, following weather predictions at 3-hour intervals. The hazard prediction results will trigger a ‘Warning’ alert in case of emergency status. This alert will be set up in a notification system to make it easier for the user to identify the most dangerous hydrometeorological hazard events.

Keywords: *extreme weather; flood; high resolution; hydrometeorology; hydro-meteorological hazard early warning system (H-MHEWS); landslide; warning; weather prediction.*

1 Introduction

Several early warning systems have been developed in Indonesia. The Indonesian Agency for Meteorology, Climatology and Geophysics (BMKG) has developed an early warning system for extreme weather that can be accessed at web.meteo.bmkg.go.id [1]. People can get predictions of thunderstorms, strong

Received November 2nd, 2017, Revised May 7th, 2018 , Accepted for publication September 12th, 2018.
 ISSN: 2337-5779, DOI: 10.5614/j.eng.technol.sci.2018.50.4.2

wind, heavy rain and high waves by accessing the website. The prediction is updated daily for weather conditions 3 days ahead, covering all of Indonesia.

Beside the system above, there is an early warning system called Satellite Disaster Early Warning System (SADEWA), which was developed by the Indonesian National Institute of Aeronautics and Space (LAPAN) and covers all of Indonesia as well. SADEWA provides weather predictions but does not yet show hazard predictions. The weather prediction is provided in 0.25° grid spatial resolution [2]. On a micro scale, flood early warning systems have already been well developed, especially for the Jakarta region. Since Jakarta is a flood prone area, the Jakarta Flood Early Warning System (J-FEWS) was built, as reported by Ginting, *et al.* [3]. These systems use an operational flood forecasting and warning system based on Delft-FEWS [4]. For landslides, the Gajah Mada University released an early warning system called LEWS (Landslide Early Warning System) using Internet-based GPS (online GPS) [5].

There is also an early warning system for high ocean waves, which was developed by the Indonesian Agency for Meteorology, Climatology and Geophysics (BMKG) and can be accessed at www.maritim.bmkg.go.id [6]. This system provides predictive information about regions that potentially have extreme waves at 24 hours ahead. This system divides the height of waves into 3 levels, i.e. moderate sea (1.25-2.5 m), rough sea (2.5-4.0 m) and very rough sea (4.0-6.0 m).

As an official institution that manages hazards, the National Disaster Management Authority (BNPB) has developed inaRISK (hazard risk index monitoring in Indonesia), which can be accessed at www.inarisk.bnpb.go.id [7]. A collection of hazard indices has been compiled in a book entitled *Indonesia Disaster Risk* [8]. The flood hazard index was obtained from an overlay method adopted from Manfreda, *et al.* [9]. Using this method, flood-prone areas are identified by modifying DEM raster data into a topographic index and then compared to a flood threshold value. The flood threshold value is obtained from flood data of major river networks. The limit of this flood hazard index is the absence of rainfall as a factor, which is usually a major trigger for flood events.

The present paper discusses the results of the development of an early warning system for hydrometeorological hazards in Indonesia (which can be accessed at mhews.bnpb.go.id) by utilizing hazard risk index monitoring (inaRISK – inarisk.bnpb.go.id) and dynamic weather prediction at 3 days ahead 3-hour intervals.

2 Methods

The prediction of hydrometeorological hazard potential can be made dynamic by overlaying the hazard index from inaRISK with weather predictions covering the whole of Indonesia. Figure 1 shows the flow of H-MHEWS development, combining two types of data, i.e. the hazard index of inaRISK and the indexed weather prediction. This scheme shows the process flow of the system, starting with numerical weather prediction (NWP) and finishing with GIS processing (calculating dynamic hazard indices) using high performance computing (HPC). Using GIS technology, H-MHEWS was developed by integrating common database operations, such as queries and statistical analysis, as well as creating visualizations and geographic analysis in the form of maps [10]. H-MHEWS is processed in GIS and all information can be linked and processed simultaneously. A syntactical expression of the changes is induced in the system by variation of the hazard index.

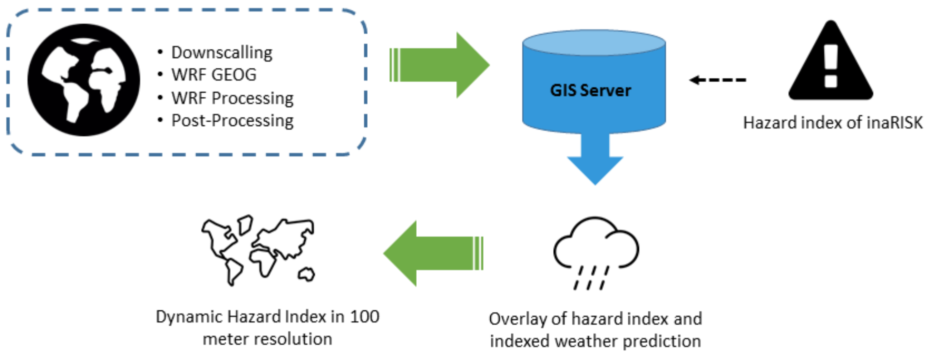

Figure 1 Flow of H-MHEWS processing.

The numerical weather prediction process using the Weather Research and Forecasting (WRF) model is described in Powers, *et al.* [11]. WRF simulations begin with the WRF Preprocessing System (WPS), a series of utilities. WPS first pulls in geographical information (e.g. topography and land use) to set up the user's model domains. As H-MHEWS needs prediction data up to 3 days ahead at 3-hour intervals, therefore this information is set up in an input configuration file called namelist.input. Next, it ingests, reformats, and interpolates the requisite first-guess atmospheric data (e.g. a global analysis or model forecast) to the user's domain. Finally, the input fields are put on the model's vertical levels and lateral boundary conditions are generated. WRF is then ready to run. This is done by the forecast component, which contains a dynamical solver and physics packages for atmospheric processes (e.g. microphysics, radiation, and planetary boundary layer). The weather prediction is processed automatically using a task scheduler in the Linux operating system [12].

A hazard index from the H-MHEWS input is obtained from inaRISK, consisting of flood hazard, landslide hazard, and an extreme weather map. Flood hazard refers to flood-prone area data and inundation depth is based on PERKA No. 2 BNPB/2012. DEM raster data are developed into flood-prone areas through topographic index modification with the following Eq. (1):

$$TI_m = \log \frac{a_d^n}{\tan(\beta)} \tag{1}$$

where TI_m is topography index modification, a_d is flow area per length contour unit (or value of the accumulated flow based on DEM data analysis, values depending on DEM resolution), tan (β) is the slope (based on DEM data analysis), and n is an exponential value; the value of n is calculated with the formula n = 0.016 x 0.46, where x is the DEM resolution.

Flood-prone areas are identified using a threshold value (T). If the topography index value is greater than a threshold value (TI_m > T), the area will be categorized as flood-prone with $T = 10.89n + 2282$. Furthermore, the flood hazard index is estimated by the slope and distance from a river at the flood-prone areas with a fuzzy method.

The second type of hazard in H-MHEWS is landslide hazard. Landslide hazard zone classification is based on the vulnerability of ground motion as issued by the Center for Volcanology and Geological Hazard Mitigation (PVMBG) and corrected for slopes above 15%. The landslide hazard index is obtained by danger area delineation after performing overlay between landslide vulnerability zone and slope analysis.

Furthermore, extreme weather hazards are divided into strong winds, heavy rainfall, and extreme ocean waves. Strong winds and heavy rainfall are obtained by scoring its constituents, which are land openness, land slope, and annual rainfall. The constituent parameters for extreme waves are wave height, ocean current, coast typology, vegetation cover, and coastline shape.

2.1 Downscaling WRF Output into 5 Km

The Weather Research and Forecasting (WRF) model is a numerical weather prediction (NWP) and atmospheric simulation system that was designed for both research and operational applications [13]. However, to make it operational, the WRF output has to be downscaled to obtain a higher resolution. In the WRF model, weather satellite data from Global Forecast System (GFS) from the National Center for Environmental Prediction (NCEP), with a resolution of 10° x 10°, is interpolated to a higher resolution by considering some parameterizations, such as microphysics, planetary boundary layer (PBL), cumulus scheme, radiation scheme, physics and dynamics options [14]. The domain is divided to have some nesting based on a regional division, with the coarse domain having a lower resolution than the term, which is done by considering domain comparison from the coarse domain to the nesting domain. In this research, downscaling was performed to increase the resolution of weather predictions to 5 km from 25 km previously (GFS data). The WRF output with 5 km spatial resolution is nested in 3 domains (see Figure 2).

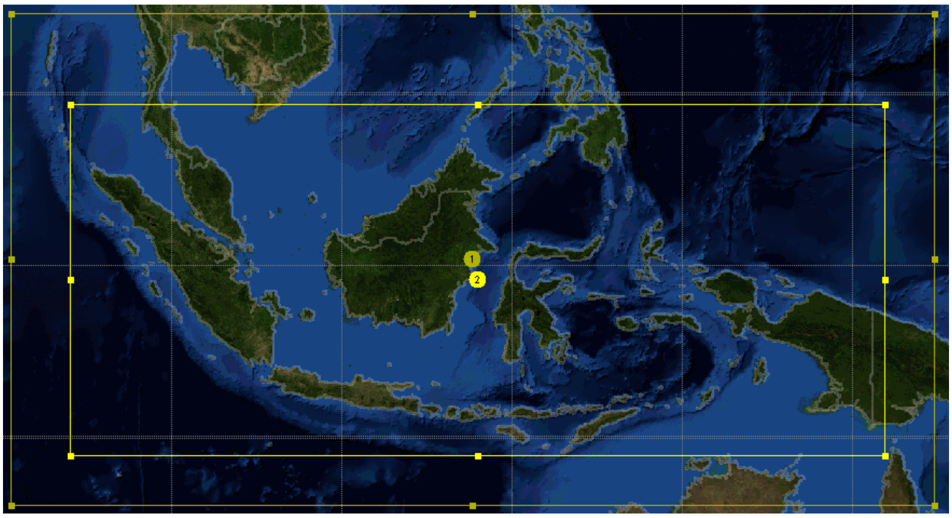

Figure 2 The domain of the H-MHEWS system.

To support the hazard index resolution, the weather prediction is generated in layers at a 100-m resolution using resampling [15]. With the resampling method, the resolution of the two data sets (inaRISK index and the indexed weather prediction) will be the same. This is because the inaRISK map provides data in 100 m resolution but weather prediction only has a 5 km resolution. The result of this resampling are weather prediction maps in raster form with a 100-m resolution.

2.2 Creating Hazard Index Prediction

A hazard index prediction map is generated by overlaying the weather prediction map with the inaRISK map. After that, an overlay map is generated as the new index representing the prediction of hazard occurrences in Indonesia. The digital hazard index and weather layers are overlaid and integrated in GIS media by raster calculator functions [16], then zoning of regions is done in 4 classes, i.e. “No alert”, “Advisory”, “Watch”, and “Warning”. The classes are applied to flood, landslide, and extreme weather hazards.

2.2.1 Flood

The flood hazard index is derived by combing the calculation and weighting of predicted rainfall with the inaRISK index. Flood hazard indices are obtained with the following Eq. (2):

$$IK = 0{,}2*IR*20 + 0{,}8*R \quad (2)$$

where:

IK : flood hazard index, the value of which will be determined to be used as the value of hazard warning
IR : flood index from inaRISK
R : amount of rainfall

Furthermore, the hazard index (IK) is classified into 4 groups, as shown in Table 1 below.

A predicted hazard index is calculated for each 100 m x 100 m grid of the domain. The index (IR) used is the hazard index from inaRISK, namely flood hazard. The amount of rainfall (R) used to calculate the hazard index is obtained from the result of weather prediction. Due to the difference in spatial resolution, the weather prediction result is resampled before combination with the hazard index. The rainfall input into the formula is the predicted rainfall resulted by the WRF model at 3-hour intervals, a resolution of 5 km, and 3 days ahead.

Table 1 Hazard indices for floods.

IK Value (Flood Hazard Index)	Status	Color
< 8	Normal	Green
8-11	Caution	Yellow
11-15	Warning	Orange
> 15	Warning	Red

For example, for an area with a flood index of 0.2 and rainfall over one time step reaching 15 mm, the hazard index values from Eq. (3) are as follows:

$$IK = 0.2 * 0.2 * 20 + 0.8 * 15 = 12.8 \quad (3)$$

Based on the table of IK values, the value of 12.8 is put into the group and will put an orange alert on the hazard warning map.

2.2.2 Landslide

The landslide hazard index is almost the same as the flood index, also derived by combining the calculations and weighting of the predicted rainfall and landslide hazard index of inaRISK. The landslide hazard indices are obtained with the following Eq. (4):

$$IK = 0,2*IR*20 + 0,8*R \quad (4)$$

where:

IK : landslide hazard index, the value of which will be determined to be used as the value of hazard warning
IR : landslide index from inaRISK
R : amount of rainfall

Furthermore, the landslide hazard index (IK) is classified into 4 groups, as shown in Table 2 below.

The landslide hazard index is calculated for each 100 m x 100 m grid of the domain. The amount of rainfall (R) that is used to calculated hazard index is obtained from the result of weather prediction by the WRF model. Due to the difference in spatial resolution, the weather prediction result is resampled before being used for the hazard index.

Table 2 Hazard indices for landslides.

IK Value (Landslide Hazard Index)	Status	Color
< 8	No Alert	Green
8-11	Advisory	Yellow
11-15	Watch	Orange
> 15	Warning	Red

For example, for an area with a flood index of 0.2 and rainfall over one time step reaching 15 mm, the hazard index values are as follows:

$$IK = 0.2 * 0.2 * 20 + 0.8 * 15 = 12.8 \quad (5)$$

Based on the table of IK values, the value of 12.8 is put into the group and will put an orange alert on the hazard warning map.

2.2.3 Heavy Rain

For the category of extreme weather, the value used is the value of the weather and maritime prediction issued by the system, henceforth it is grouped into several categories. Predictions for heavy rain are grouped into the following 4 hazard groups (Table 3).

Table 3 Index and status of heavy rain.

Rainfall	Status	Color
< 5 mm	No Alert	Green
5-10 mm	Advisory	Yellow
10-20 mm	Watch	Orange
> 20 mm	Warning	Red

For example, if the rainfall in an area is 18 mm in one time step, then the area's alert status at that time is extreme weather and heavy rain. It will be made orange on the map of extreme weather warnings, showing heavy rain.

2.2.4 Strong Winds

In the system of early warning for strong winds, the predicted wind speeds are grouped into the following 4 groups as (Table 4).

Table 4 Index and status of strong winds.

Velocity	Status	Color
< 3 m/s	No Alert	Green
3-5 m/s	Advisory	Yellow
5-8 m/s	Watch	Orange
> 8 m/s	Warning	Red

For example, if the wind speed in an area is 9 m/s in one time step, then the area's alert status at that time is extreme weather and strong winds. It will be colored red on the map of extreme weather.

2.2.5 Extreme Ocean Waves

The ocean wave height parameter used in the prediction is significant wave height, which is defined as the average height of the highest one-third waves in the wave spectrum [17]. Predictions of extreme hazard at high tide are divided into 4 groups as shown in Table 5 below. The predicted ocean wave heights result from the SWAN (Simulating Waves Nearshore) model. SWAN is a third-generation wave model that can be used for small-scale coastal regions with shallow water, (barrier) islands, tidal flats, local wind, and ambient currents [18].

Table 5 Index and status of extreme ocean waves.

Wave	Status	Color
< 0.50 m	No Alert	Green
0.50-1.25 m	Advisory	Yellow
1.25-1.50 m	Watch	Orange
> 1.50	Warning	Red

3 Results

High-resolution mapping of weather predictions is important in hazard prediction. This is because extreme weather conditions, especially rainfall, are often the largest triggers of hydrometeorological disasters. H-MHEWS provides high-resolution and high-accuracy weather predictions. The weather forecast has a spatial resolution of 5 km with prediction at 3 days ahead and a 3-hour temporal resolution.

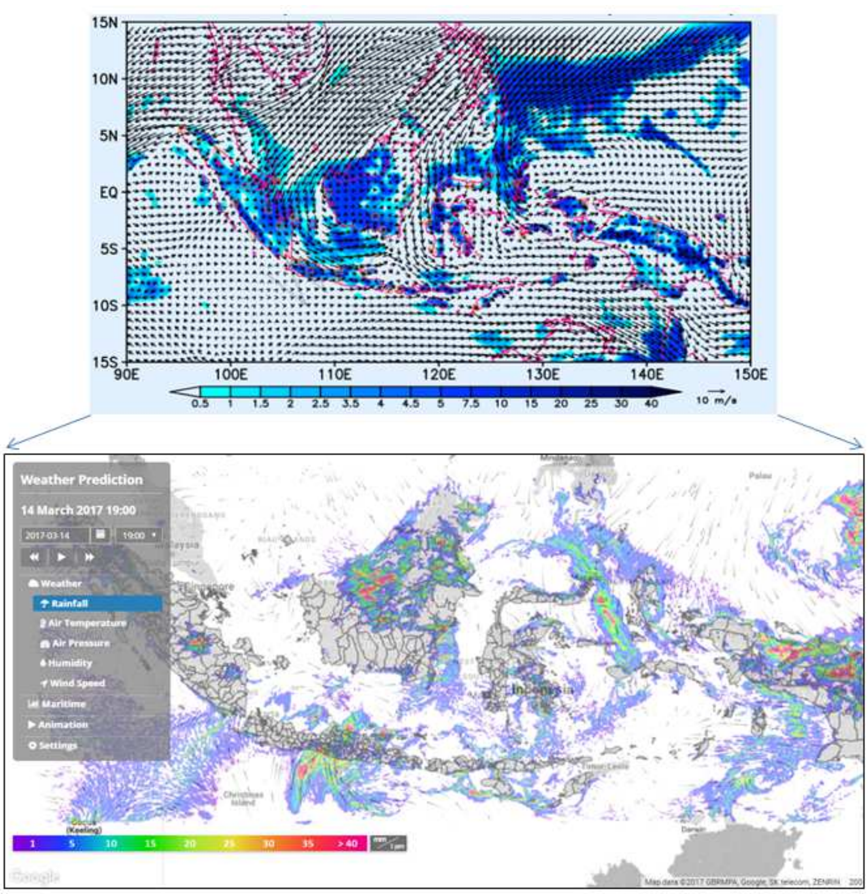

Figure 3 Upgrading weather prediction resolution to 5 km.

In the first development phase, the weather prediction plot of H-MHEWS used static images based on the Grid Analysis and Display System (GraDS) output. However, in the current development phase, the weather prediction of H-MHEWS is made more dynamic by adding a form of wind animation in JSON format on the website. This format allows the user to see the wind displacement direction dynamically (Figure 3).

In the process described previously, there is a need to make an overlay of the inaRISK hazard index and the dynamic weather prediction map to produce an hazard index prediction at 3 days ahead. BNPB has made a hazard index for floods, landslides, and extreme weather events as shown in Figure 4. The green color indicates areas with 'No alert' predicted weather, yellow means 'Advisory, orange means 'Watch' and red means 'Warning'. This index is based on the following classification.

Table 6 Index and status of inaRISK hazard vulnerability.

Index	Status	Color
0-0.25	No Alert	Green
0.25-0.5	Advisory	Yellow
0.5-0.75	Watch	Orange
0.75-1	Warning	Red

For example, if an area has a hazard landslide index of 0.3, then the area will be colored yellow on the index prediction map for landslides.

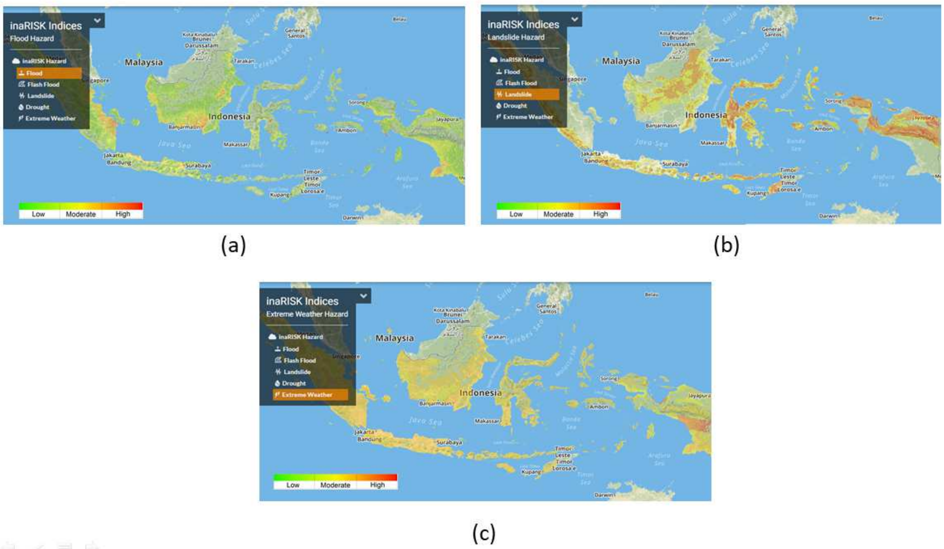

Figure 4 Hazard index from inaRISK: (a) flood, (b) landslide, (c) extreme weather.

Furthermore, the result is overlaid with weather predictions along with inaRISK hazard prediction. The result of the map overlay generates a new index that represents the potential hazard prediction for Indonesia so that mitigation can be done quickly and accurately. The map overlay of inaRISK and weather predictions is done in an attempt to form hazard indices that can be displayed in decision support systems (DSS) on websites. The hazard indeces indicate the status of an area at a predetermined time, i.e. 'No alert', 'Advisory', 'Watch', and 'Warning'. Both the hazard index and the inaRISK index made with the existing methods can be permanently displayed to be able to constantly monitor the results and validate them with data from the field.

Figure 5 shows examples of flood hazard predictions at 3 local times. Figure 5(a) shows predictions of hazards for 15 February 2017 at 10.00. This image shows which areas are red, i.e. 'Warning' status, orange, i.e. 'Watch' status, yellow, i.e. 'Advisory' status, i.e. green, i.e. 'No alert' status for floods. Figure 5(b) contains information regarding the status of flooding but at different local times. Figure 5(a) shows it at 10.00, Figure 5(b) is at 13.00, and Figure 5(c) is at 16.00. It can be seen that the changes will continue over time to follow the variation of the predicted weather.

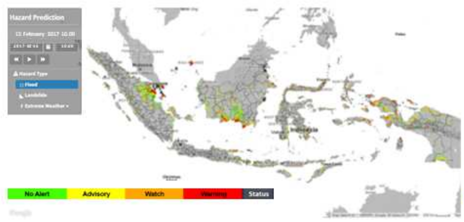

(a)

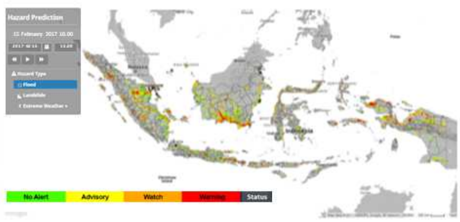

(b)

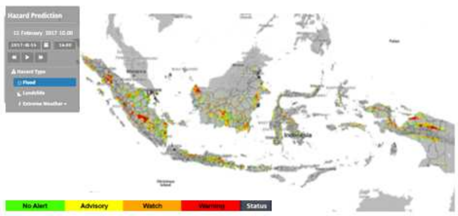

(c)

Figure 5 Prediction of flood hazard on 15 February 2017: (a) at 10.00 LT, (b) at 13.00 LT, (c) at 16.00 LT.

Figure 6 shows examples of landslide hazard predictions at 3 local times. Figure 6(a) shows hazard predictions for 15 February 2017 at 10.00 LT. This image describes the hazard index made from an overlay of the weather prediction and the landslide index. Figure 6(b) contains information regarding the status of flooding but at a different local time. Figure 6(a) is at 10.00, Figure 6(b) is at 13.00, and Figure 6(c) is at 16.00.

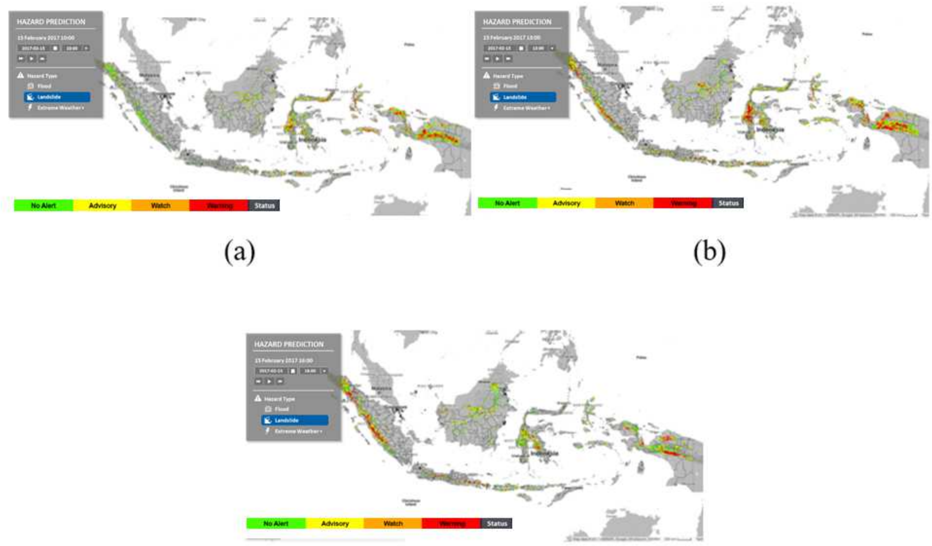

(a) (b)

(c)

Figure 6 Prediction of landslide hazard index on 15 February 2017: (a) at 10LT, (b) at 13LT, (c) at 16LT.

Figure 7 shows the hazard prediction for extreme rainfall at 3 different times. Figure 7(a) shows which areas 15 February 2017 10.00 are categorized as 'Warning' (red in the maps), 'Advisory' (orange in the maps), 'Watch' (yellow in the maps), and 'No Warning' (green in maps). Figure 7(b) shows the same as Figure 7(a) but at a different local time, 13.00, and Figure 7(c), 16.00. The extreme weather index is obtained from determination of the weather parameter prediction for rainfall, wind speed, and wave.

The simulation results in hazard prediction can be displayed in a DSS in the form of a website, which makes it easier for the user to read the results of hazard prediction and facilitate decision-making for mitigation purposes. On this website, there is also a map that contains the warning status for hazards in Indonesia. A visualization of a DSS on the website can be seen in Figure 8.

The map loads a simulated 'Advisory' alert that allows users to quickly find any hazard coming to a specified zone. In this map, there is the option to overlay weather maps, for example rainfall and wind speed. In addition, there is an option to download an Excel file that contains the information on hazard alerts in all regions in Indonesia.

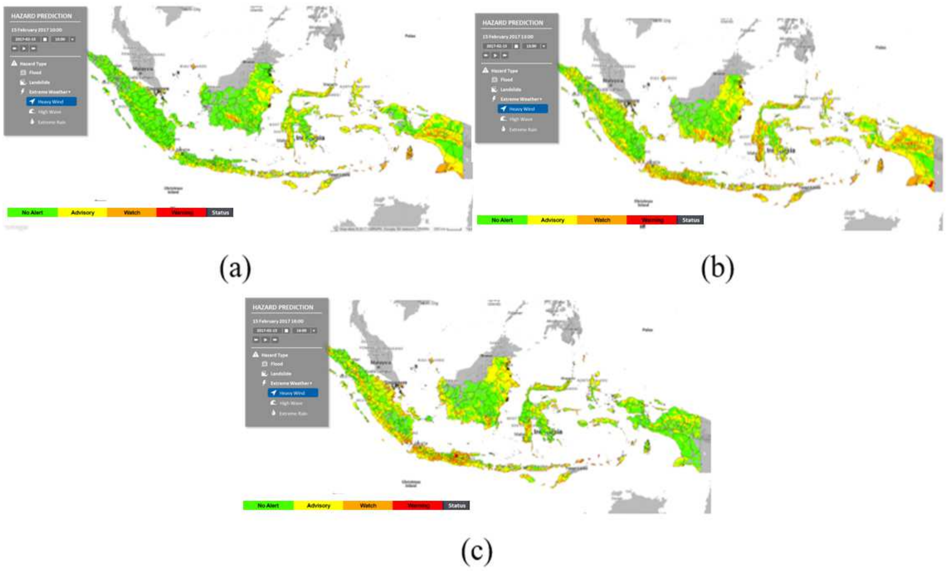

Figure 7 Prediction of extreme weather hazard index on 15 February 2017: (a) at 10.00 LT, (b) at 13.00 LT, (c) at 16.00 LT.

Figure 8 Landslide warning on 15 February 2017 at 10.00 LT.

Figure 9 shows an example of the hazard alert information in CSV format. The file provides information on the province, status ('Advisory' and 'Warning'), regency, and village regarding potential hazard events at 3 days ahead and 3-

hour intervals. This also has the purpose of facilitating the user to evaluate and validate the prediction information based on real conditions.

Early Warning of Hydro-Meteorological Hazards					
Hazard type:		FLOOD			
Date:		3/23/2018			
Time:		13			
NO	PROVICE	DISTRICT	SUB-DISTRICT	VILLAGE	ALERT STATUS
1	RIAU	INDRAGIRI_HILIR	KATEMAN	AIR_TAWAR	Warning
2	RIAU	INDRAGIRI_HILIR	KATEMAN	BANDAR_SRI_GEMILANG	Warning
3	RIAU	INDRAGIRI_HILIR	PULAU_BURUNG	PULAU_BURUNG	Warning
4	RIAU	INDRAGIRI_HILIR	PULAU_BURUNG	SUNGAI_DANAI	Warning
5	RIAU	INDRAGIRI_HILIR	PULAU_BURUNG	SRI_DANAI	Warning
6	RIAU	PELALAWAN	KUALA_KAMPAR	SUNGAI_SOLOK	Warning
7	RIAU	PELALAWAN	KUALA_KAMPAR	SUNGAI_UPIH	Warning
8	RIAU	S_I_A_K	SUNGAI_APIT	TANJUNG_KURAS	Warning
9	RIAU	S_I_A_K	SUNGAI_APIT	KAYU_ARA_PERMAI	Warning
10	RIAU	BENGKALIS	BUKIT_BATU	PARIT_I_API_API	Warning
11	RIAU	BENGKALIS	BUKIT_BATU	SEPAHAT	Advisory
12	RIAU	BENGKALIS	RUPAT	TERKUL	Advisory
13	RIAU	BENGKALIS	RUPAT	SEI_CINGAM	Warning
14	RIAU	BENGKALIS	RUPAT	PANGKALAN_NYIRIH	Warning
15	RIAU	BENGKALIS	RUPAT	MAKERUH	Warning
16	RIAU	BENGKALIS	RUPAT	DARUL_AMAN	Warning
17	RIAU	BENGKALIS	RUPAT_UTARA	TITI_AKAR	Warning
18	RIAU	BENGKALIS	RUPAT_UTARA	TANJUNG_MEDANG	Warning

Figure 9 Output of hazard alert information in CSV format.

4 Discussion and Analysis

H-MHEWS is an operational system of BNPB to monitor disaster events in Indonesia. To keep the system accurate and ensure that it matches real conditions, its data are continuously compared with real events in Indonesia collected by BNPB. Based on the first evaluation in 2016, almost all parameters provided in H-MHEWS, such as floods, landslides, extreme weather events and rainfall alerts had a good match with real event data. The comparison result can be seen in Table 6, which shows correlations that BNPB detected between H-MHEWS output and observation data.

The skill score of high-resolution weather prediction in regions around Java Island has been discussed by Fachrizal [20]. At 1:1 resolution, the skill score of high-resolution weather prediction is able to reach an accuracy of 0.8. Although the skill score is high, H-MHEWS still has uncertainty in its results that should be identified in future research.

Table 7 Comparison between H-MHEWS output and observation data [19].

Parameter	Comparison Test with Real Event
Landslide	60%
Flood	75%
Extreme weather	80%
Rainfall	86%

Regarding this prediction uncertainty, the World Meteorological Organization [21] states that even the most sophisticated numerical weather prediction systems still have uncertainty and are able to produce wrong predictions. The chaotic nature of the atmosphere, as stated by Lorenz [22], and the parameterization scheme in numerical weather prediction, as stated by Buizza [23], are the two main sources of uncertainty in numerical weather prediction. Hence, they will also affect the accuracy of H-MHEWS.

Several methods are available to reduce the uncertainty of H-MHEWS. The first is to assimilate ground observation data or radar/satellite observation data. Kumar, *et al.* [24] have shown that satellite rainfall data are able to improve the rainfall result of weather predictions. Besides data assimilation, ensemble prediction systems are also able to solve uncertainty problems in weather prediction, as stated by Buizza, *et al.* [25]. Ensemble prediction systems are able to produce probabilistic forecasts, as stated by Joslyn and Savelli [26] and Joslyn and Le Clerc [27], which is beneficial for the user. Pratama [28] has tried using an ensemble method to reduce uncertainty of rain prediction in Bandung, West Java, with satisfactory results.

In the future, these hazard prediction methods will continue to be developed to improve the quality of H-MHEWS. Therefore, the development of increased accuracy in prediction, the development of the website, and validation of the results of hazard prediction will be continued to increase the benefits of H-MHEWS.

5 Conclusions

Society requires hydrometeorological hazard early warning information to see potentially dangerous weather patterns in advance. This research produced the information needed by the community in the form of predictive hydro-meteorological hazards at 3 days ahead and intervals of 3 hours with a 5 km spatial resolution. This information can be accessed at mhews.bnpb.go.id. It is used in a DSS in the form of a website that informs the user which areas have a hazard warning. The DSS provides the most important information in a user-friendly way as a service to society.

Acknowledgements

We thank the National Disaster Management Authority (BNPB), Indonesia for their support of the authors and their contribution to H-MHEWS development and access to the services of inaRISK. The publication of this paper was supported by the Ministry of Research, Technology and Higher Education of the Republic of Indonesia.

References

[1] *Meteorological, Climatology and Geophysics Agency (BMKG*), Warning map from http://web.meteo.bmkg.go.id/id, retrieved 27 October 2017.

[2] Purwalaksana, A.Z. & Waslaluddin, S., *Automation from the Results of Automatic Weather Station (AWS) Observation and Its Utilization of Satellite Disaster Early Warning System (SADEWA)*, Fibusi (JoF), **3**(3), pp. 1-8 December 2015.

[3] Ginting, S. & Adidarma, W., *Jakarta Flood Early Warning System (J-FEWS)*, Workshop on MCCOE Radar Meteorology/Climatology in Indonesia, 2013.

[4] Hatmoko, W., Radhika, Raharja, B., Tollenaar, D. & Vernimmen, R., *Monitoring and Prediction of Hydrological Drought Using a Drought Early Warning System in Pemali-Comal River Basin, Indonesia*, Procedia Environmental Sciences, **24**, pp. 56-64, 2015.

[5] Aditya, T., Suharyanto, Karnawati., D. & Fathani, T.F., *Development of Landslide Early Warning System by Online GPS in Central Java, Indonesia*, Proceeding of International Symposium and The 2nd AUN/Seed-Net Regional Conference on Geo-Disaster Mitigation in ASEAN, pp. 225-234, 2010.

[6] Meteorological, Climatology and Geophysics Agency (BMKG), *Wave Height Warning Information,* accessed from , 27 October 2017.

[7] InaRISK (Hazard Risk Index Monitoring in Indonesia) from www.inarisk.bnpb.go.id, 27 October 2017.

[8] National Disaster Management Authority, *Indonesia Disaster Risk*, 2016.

[9] Manfreda, S., Leo, M.D., Sole, A. *Detection of Flood-Prone Areas Using Digital Elevation Models*, Journal of Hydrologic Engineering, **16**(10), pp. 781-790, doi: 10.1061/(ASCE)HE.1943-5584 .0000367.

[10] Burrough, P.A., *Principles of Geographical Information System for Land Resources Assessment*, Oxford University Press, Oxford, 1990.

[11] Powers, J.G., Klemp, J.B., Skamarock, W.C., Davis, C.A., Dudhia, J., Gill, D.O., Coen, J.L., Goghis, D.J., Ahmadov, R., Peckham, S.E., Grell, G.A., Michalakes, J., Trahan, S., Benjamin, S.G., Alexander, C.R., Dimego, G.J., Wang, W., Schwartz, C.S., Romine, G.S., Liu, Z., Snyder, C., Chen, F., Barlage, M.J., Yu, W. & Duda, M.G., *The Weather Research and Forecasting Model: Overview, System Efforts, and Future Directions*, Bulletin of American Meteorological Society, August 2017, **98**(8), pp. 1717-1737, 2017.

[12] Keller, M.S. *Cron Job Scheduler*, Linux Journal, Sep 01 1999. https://www.linuxjournal.com/article/3290, retrieved 27 October 2017.

[13] Skamarock, W.C., Klemp, J.B., Dudhia, J., Gill, D.O., Barker, D.M., Wang, W. & Powers, J.G., *A Description of the Advanced Research WRF*

version 2, National Center for Atmospheric Research, Technical Note, NCAR/TN-468þSTR. (Boulder, CO), 2005.

[14] National Center for Atmospheric Research, *The Advanced Research WRF (ARW) Version 3.4 Modeling System*, Released in April 2012.

[15] Usery, E.L., Finn, M.P., Scheidt, D.J., Ruhl, S., Beard, T. & Bearden, M. *Geospatial Data Resampling and Resolution Effects on Watershed Modeling: A Case Study using the Agricultural Non-point Source Pollution Model*, Journal of Geographical System, **6**, pp. 289-306, 2004, doi: 10.1007/s10109-004-0138-z.

[16] Nasrollahi, N., Kazemi, H. & Kamkar, B., *Feasibility of Ley-Farming System Performance in a Semi-Arid Region using Spatial Analysis*, Journal of Ecological Indicators, **72**, pp. 239-248, 2017.

[17] Ainsworth, T., *When Do Ocean Waves Become 'Significant'? A Closer Look at Wave Forecasts*, Mariners Weather Log, **50**(1), April 2006.

[18] Thomas, T.J. & Dwarakish, G.S., *Numerical Wave Modelling-A Review*, Aquatic Procedia, **4**, pp. 443-448, 2015.

[19] BNPB Team, *Evaluation of MHEWS Parameter with Observation Data*, BNPB Report, 2016.

[20] Fachrizal, F., *Verification of Numerical Weather Prediction with Neighborhood Method*, Undergraduate Theses, Institut Teknologi Bandung, Indonesia, 2017. (Text in Indonesian)

[21] World Meteorological Organization, *Guidelines on Ensemble Prediction Systems and Forecasting*, Geneva: World Meteorological Organization, 2012.

[22] Lorenz, E.N., *Deterministic Nonperiodic Flow*, Journal of the Atmospheric Science, **20**(2), pp. 130-141, 1963.

[23] Buizza, R., *The ECMWF Ensemble Prediction System in T. Palmer, & R. Hagedorn, Predictability of Weather and Climate*, Cambridge: Cambridge University Press, pp. 459-488, 2006, ISBN: 9780511617652.

[24] Kumar, P., Kishtawal, C.M. & Pal, P.K., *Impact of Satellite Rainfall Assimilation on Weather Research and Forecasting Model Predictions Over the Indian Region*, Journal of Geophysical Research: Atmospheres, **119**(5), pp. 2017-2031, 2014.

[25] Buizza, R., Houtekamer, P.L., Toth, Z., Pellerin, G., Wei, M. & Zhu, Y., *A Comparison of the ECMWF, MSC, and NCEP Global Ensemble Prediction Systems*, Monthly Weather Review, **133**(5), pp. 1076-1097, 2005, doi:10.1175/MWR2905.1.

[26] Joslyn, S. & Savelli, S., *Communicating Forecast Uncertainty: Public Perception of Weather Forecast Uncertainty*, Royal Meteorology Society, **17**(2), pp. 180-195, 2010.

[27] Joslyn, S.L. & LeClerc, J.E., *Uncertainty Forecast Improve Weather-Related Decisions and Attenuate the Effects of Forecast Error,* Journal of

Experimental Psychology: Applied, **18**(1), pp. 126-140, 2012, doi: 10.1037/a0025185.

[28] Pratama, A. F., *Probabilistic Prediction in Bandung using Ensemble Prediction System*, Research Report, Institut Teknologi Bandung, 2017. (Text in Indonesian)